Proceedings of the 2nd Winter Workshop S&SRES'96, Polanica Zdrój 1996

ENERGY TRANSFER AND UP-CONVERSION IN THE ERBIUM ELPASOLITES $Cs_2NaEr_xY_{1-x}Cl_6$

M. CAMPBELL AND C.D. FLINT

Laser Laboratory, Department of Chemistry, Birkbeck College, University of London
29 Gordon Square, London, WC1H 0PP, U.K.

The luminescence decay curves from the $^4F_{9/2}$ and $^4I_{9/2}$ states of the cubic hexachloroelpasolite crystals $Cs_2NaEr_xY_{1-x}Cl_6$ ($x = 0.001 \div 1$) have been measured over the temperature range 10–300 K. The $^4I_{9/2}$ state undergoes an electric dipole vibronic–electric dipole vibronic cross-relaxation process at 300 K, but this mechanism is inefficient below 165 K. Excitation into the $^4F_{9/2}$ state, results in emission in the green, blue and ultra violet regions. The up-conversion processes which could account for the ultraviolet emission are discussed.

PACS numbers: 13.40.Hq, 31.70.Hq, 34.30.+h, 61.72.Ss, 78.55.Hx

1. Introduction

The cubic erbium hexachloroelpasolite is a useful system for the study of energy transfer processes for a number of reasons. Firstly, the erbium ions occupy sites of exact octahedral symmetry and consequently pure electric dipole radiative f–f transitions are forbidden. Overall f–f transition probabilities (from magnetic dipole and vibronic transitions) are relatively small.

This leads to long lived excited states and therefore facilitates the observation of energy transfer processes. Secondly, in the elpasolite lattice, the phonon cut-off frequency is smaller than 300 cm^{-1}. This reduces the non-radiative transition rates between levels and therefore luminescence is observed from many excited states. Thirdly, the octahedral crystal field means that the number of crystal field levels is minimized. This lowers the number of possible interaction pathways leading to energy transfer processes and allows the mechanisms to be determined more precisely.

The energy levels of erbium both, as a free ion and in the elpasolite lattice, have been extensively investigated and are well catalogued [1, 2]. The odd parity vibrational modes of the $ErCl_6^{3+}$ moiety, ν_6, ν_4 and ν_3, occur at about 80, 120, and 280 cm^{-1} and are readily observed in the vibronic transitions. There are a large number of higher energy levels of Er^{3+} in the visible and near infrared regions (Fig. 1), many having similar energy gaps between them. This ladder like structure, coupled with the fact that these states can be extremely long lived

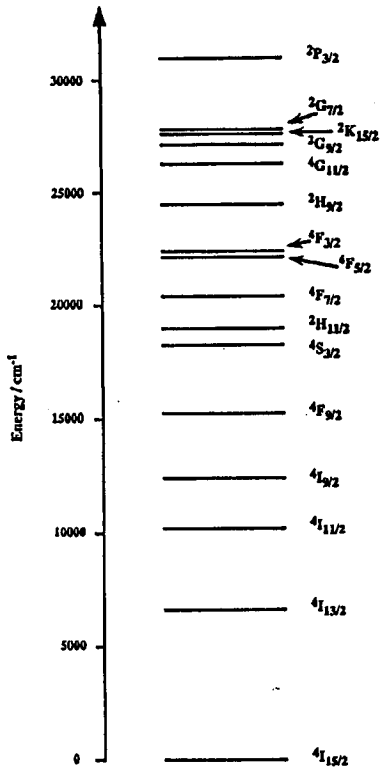

Fig. 1. Energy levels of Er^{3+}.

means that there are a large number of energy transfer possibilities which may lead to cross relaxation and up-conversion processes.

In this paper we present the decay kinetics of the $^4F_{9/2}$ and $^4I_{9/2}$ states of this system, and the up-conversion processes resulting from the population of these states which have not been reported previously [3,4].

2. Experimental

Luminescence decay curves were measured from single crystals of $Cs_2NaEr_xY_{1-x}Cl_6$, synthesized using a modified Bridgman method, as described previously [5]. Excitation was into the $^4F_{9/2}$ state at 15360 cm^{-1} and decay curves were measured over the temperature range 10–300 K and for the concentration range $x = 0.001 \div 1.0$. The emission from the $^4I_{9/2}$ state is conspicuously long lived (lifetime > 0.1 s at low temperatures in dilute samples) and it is necessary therefore to use very low laser pulse repetition rates (< 2 s^{-1}) if excited state absorption of a second laser pulse is to be avoided.

3. Decay of excited $^4F_{9/2}$ states

The luminescence decay curves of the $^4F_{9/2}$ state were measured at 14950 cm^{-1} (the $^4F_{9/2} \rightarrow {}^4I_{15/2}$ transition) and were exponential for all concentrations and temperatures. At 300 K the decay constants are almost independent of concentration (Fig. 2). At lower temperatures, the decay constant decreases and becomes dependent on the concentration. At low temperatures there are no two-ion, two phonon cross-relaxation processes available, so cross relaxation will be inefficient. At the lowest concentrations, when the erbium ions are effectively separated from one another, the change in the decay constant with temperature (Fig. 3) is consistent with the coth law for vibronic transitions, although the thermal population of different components of the $^4F_{9/2}$ state will also contribute to this temperature dependence. The concentration dependence occurs rather abruptly between $x = 0.15$ and $x = 0.25$, in this concentration range almost every erbium ion has at least one other erbium ion as a nearest neighbour and it is likely that energy migration amongst the donor ions is responsible for the change in behaviour. This would be consistent with the exponential decay curves at intermediate values of x.

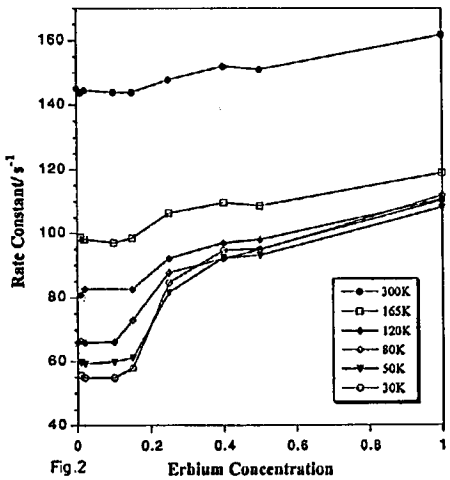

Fig.2

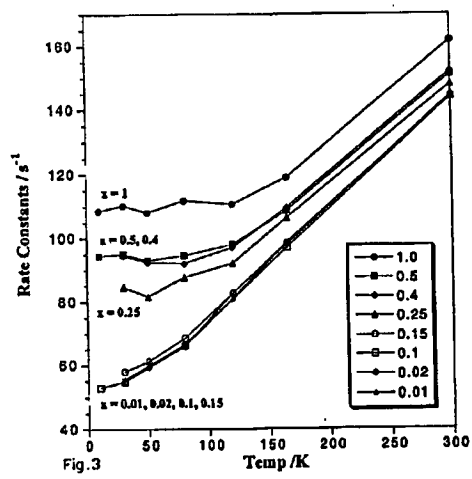

Fig.3

Fig. 2. The concentration dependence (erbium mole fraction) of the decay constants of the excited $^4F_{9/2}$ state (measured at 14950 cm^{-1}) for $Cs_2NaEr_xY_{1-x}Cl_6$ at various temperatures.

Fig. 3. The temperature dependence of the decay constants of the excited $^4F_{9/2}$ state of $Cs_2NaEr_xY_{1-x}Cl_6$ (measured at 14950 cm^{-1}) for various mole fractions of erbium.

4. Decay of the excited $^4I_{9/2}$ states

The $^4I_{9/2}$ state of erbium is populated by decay from the $^4F_{9/2}$ state, the energy gap between these two levels being approximately 2650 cm^{-1} which corresponds to about 9 of the highest energy vibrations in this lattice. The non-radiative transition between the two states is therefore expected to be relatively unimportant and the $^4I_{9/2}$ can be assumed to be populated predominantly by the radiative

transition from the $^4F_{9/2}$ state. As expected the luminescence decay curves (measured at 12240 cm^{-1}) show a slow rise with a constant equal to the decay constant of the $^4F_{9/2}$ state followed by a conspicuously slow exponential decay.

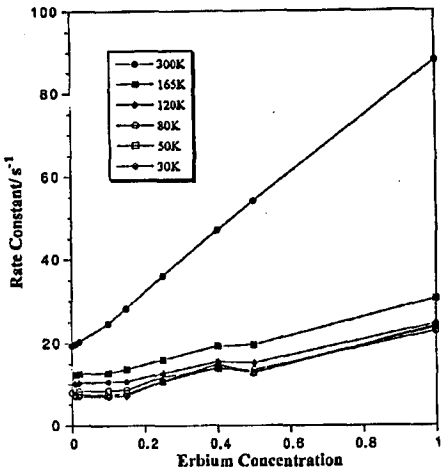

Fig. 4. The concentration dependence (erbium mole fraction) of the decay constants of the excited $^4I_{9/2}$ state (measured at 12240 cm^{-1}) of $Cs_2NaEr_xY_{1-x}Cl_6$ for different temperatures.

At low temperatures (< 165 K) there is only a slight concentration quenching occurring (Fig. 4). At higher temperatures there is an almost linear increase in the decay rate constant with concentration. This is attributed to the cross-relaxation mechanism

$$^4I_{9/2} + {}^4I_{15/2} + \nu_u \rightarrow {}^4I_{13/2} + {}^4I_{13/2} + \nu'_u.$$

This mechanism requires the thermal population of higher crystal field levels as well as the absorption of a phonon on either or both the donor and acceptor levels. A distribution over these levels is consistent with the observed temperature dependence.

The shell model describing the decay of the donor emission in the presence of acceptors may be written [6]

$$I(t) = I(0)\exp(-k_0 t) \prod_{r_n}^{\text{all shells}} \sum_{r_n}^{N_n} O_{r_n}^{N_n}(x) \exp\left[-r_n \left(\frac{R_1}{R_n}\right)^6 k^{ET} t\right],$$

where x is the mole fraction of acceptors, k_0 is the intrinsic decay of the isolated ion, N_n is the maximum number of ions in the n-th shell, r_n is the occupancy factor, $O_{r_n}^{N_n}(x)$ is the probability of a particular distribution of acceptors, R_1/R_n the ratio of the distance of the nearest neighbour shell to the n-th shell, and k^{ET} is the energy transfer rate to a single ion at the nearest neighbour position. It can be shown [6] that for the $x = 1$ case (i.e. 100% erbium) the decay is exponential with a decay of $k_0 + 14.42k^{ET}$. Using this relationship (which also applies in the

presence of migration amongst the donors) we find that $k^{ET} = 4.6\ s^{-1}$ at 300 K. Although this is a very slow rate of energy transfer, it is observable due to the extremely long lifetime of the $^4I_{9/2}$ state which is 51.5 ms ($k = 19.4\ s^{-1}$) for the isolated ion at 300 K and 151.5 ms at 10 K ($k = 6.6\ s^{-1}$).

5. Up-conversion processes

Under red excitation, emission was also observed at shorter wavelength than the exciting wavelength, with luminescence occurring in the ultraviolet, blue and green regions at 25975, 24100, 22075, 20410 and 17860 cm^{-1}. The emission at 25975 cm^{-1} which is the subject of this paper was approximately 4 or 5 times more intense than that at 24100 cm^{-1} and at least two orders of magnitude greater than the other emissions. The time evolution of the lower states populated by up-conversion is more complex and will be discussed elsewhere.

A study of the power dependence of the emission intensity at 25975 cm^{-1} gives a quadratic dependence upon the input laser power implying a two-photon mechanism for this red to ultraviolet up-conversion. The only possible excited state for this emission is then the $^4G_{11/2}$ and the up-conversion must involve the $^4F_{9/2}$ state. For $x = 1$ the luminescence decay curve shows a slow rise (5 ms at 80 K) at all temperatures, but for $x = 0.1$ a much faster (but clearly observable, 200 μs at 80 K) rise occurs at all temperatures. At intermediate concentrations there is a monotonic transition between these two types of behaviour. The contributions of these two processes are temperature dependent (Figs. 5, 6, 7).

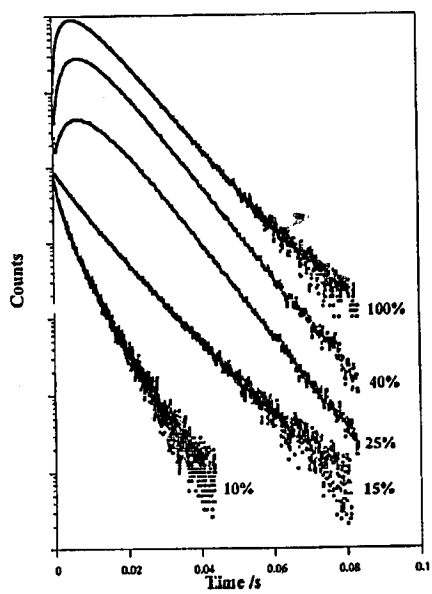

Fig. 5. 80 K ultraviolet luminescence decay curves (measured at 25974 cm^{-1}) with excitation at 15360 cm^{-1} for various mole fractions of erbium in $Cs_2NaEr_xY_{1-x}Cl_6$.

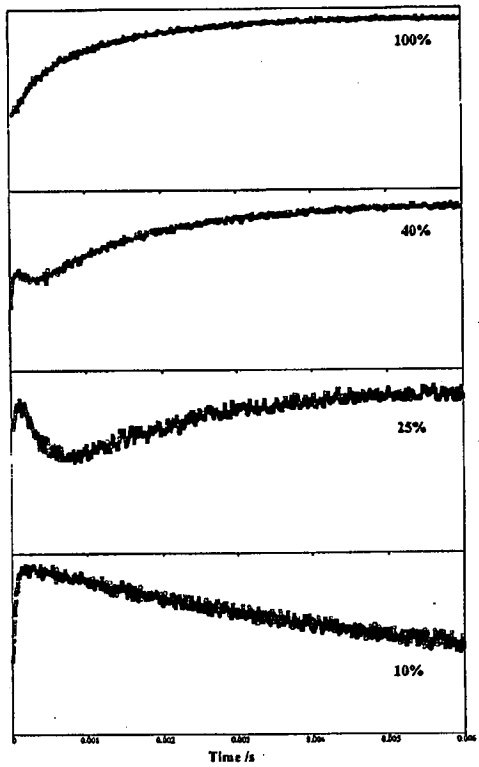

Fig. 6. Initial components of the 80 K ultraviolet luminescence decay curves (measured at 25974 cm^{-1}) with excitation at 15360 cm^{-1} for various mole fractions of erbium in $Cs_2NaEr_{0.1}Y_{0.9}Cl_6$.

Processes which might contribute to emission from the $^4G_{11/2}$ state include:

(1) Energy transfer from one excited ion to another already excited ion

$$^4F_{9/2} + {}^4I_{9/2} \rightarrow {}^4I_{15/2} + {}^2K_{15/2}$$

followed by fast relaxation from the $^2K_{15/2}$ level to the $^4G_{11/2}$.

(2) Energy transfer from one excited ion to another already excited ion

$$^4F_{9/2} + {}^4F_{9/2} \rightarrow {}^4I_{15/2} + {}^2G_{7/2}$$

followed by fast relaxation from the $^2G_{7/2}$ level to the $^4G_{11/2}$.

(3) Excited state absorption from the $^4F_{9/2}$ state excited during the same laser pulse leading to population of the $^2G_{7/2}$ level followed by fast relaxation from the $^2G_{7/2}$ level to the $^4G_{11/2}$.

If we assume fast migration amongst the donors and restrict energy transfer to nearest neighbour interactions (within the shell model 83% of the energy transfer process occur between nearest neighbours for dipole– dipole interactions) then the rate equations describing the populations of these levels for Process (1) are

$$\frac{dn_3}{dt} = Xn_1 - k_3n_3 - Wn_3n_2, \tag{1}$$

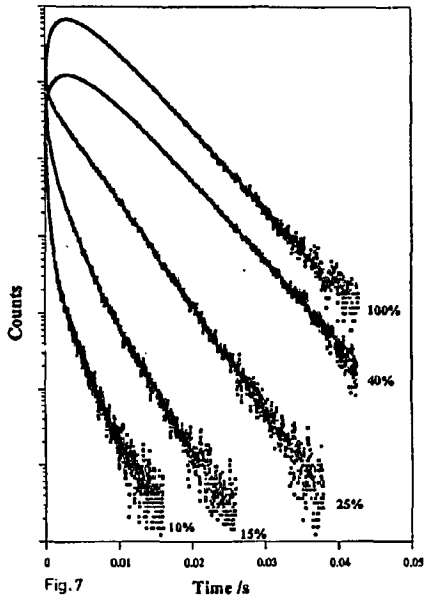

Fig. 7

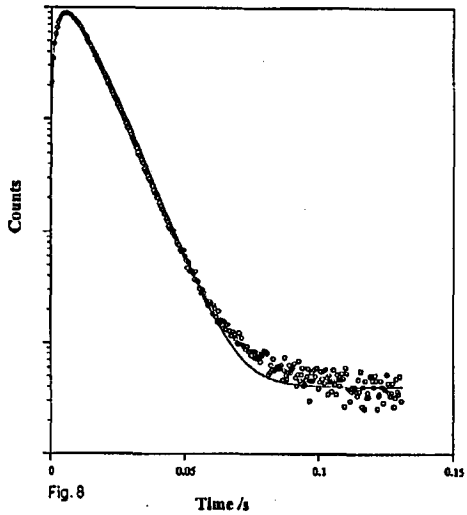

Fig. 8

Fig. 7. 300 K UV luminescence decay curves (measured at 25974 cm^{-1}) with excitation at 15360 cm^{-1} for various mole fractions of erbium in $Cs_2NaEr_{0.1}Y_{0.9}Cl_6$.
Fig. 8 80 K ultraviolet luminescence decay curves (measured at 25974 cm^{-1}) with excitation at 15360 cm^{-1} for $Cs_2NaErCl_6$. The solid line was calculated a priori using Eq. (6).

$$\frac{dn_2}{dt} = \zeta k_3 n_3 - k_2 n_2 - W n_3 n_2, \tag{2}$$

$$\frac{dn_4}{dt} = 2W n_3 n_2 - k_4 n_4, \tag{3}$$

where the levels $^4I_{15/2}$, $^4I_{9/2}$, $^4F_{9/2}$ and $^4G_{11/2}$ are labelled 1, 2, 3 and 4, respectively and k_i is the intrinsic decay constant for the i-th level and n_i is the population of the i-th level. X is the rate of excitation of the erbium ions and is the product of Er^{3+} absorption cross section and the incident photon flux and W is the rate of energy transfer leading to the up-conversion. ζ is the branching ratio for the transition to the $^4I_{9/2}$ state.

The acceptor is excited to the $^2K_{15/2}$ state from which rapid thermal relaxation occurs to the $^4G_{11/2}$ state which is responsible for the luminescence at about 25975 cm^{-1}. Therefore, in the preceding rate equations, the terms for back transfer have been neglected since they will be extremely small. The re-population of the $^4F_{9/2}$ and $^4I_{9/2}$ states from the higher energy $^4G_{11/2}$ state has been neglected.

To obtain an approximate analytical solution to these coupled nonlinear differential equations, the last terms in Eqs. (1) and (2) are assumed to be relatively small and are neglected. For a δ function pulse at time zero the approximate solutions are

$$n_3(t) = n_3(0)\exp(-k_3 t), \tag{4}$$

$$n_2(t) = \frac{n_3(0)\zeta k_3}{k_2 - k_3}\left[\exp(-k_3 t) - \exp(-k_2 t)\right], \tag{5}$$

$$n_4(t) = \frac{2n_3(0)^2 W\zeta k_3}{k_2 - k_3} \times \left[\frac{\exp(-2k_3 t) - \exp(-k_4 t)}{k_4 - 2k_3} + \frac{\exp(-k_4 t) - \exp(-k_3 - k_2)t}{k_4 - k_3 - k_2}\right]. \tag{6}$$

Similarly, it is possible for the up-conversion to occur via Process (2)

$$\frac{dn_3}{dt} = Xn_1 - k_3 n_3 - Wn_3 n_3, \tag{7}$$

$$\frac{dn_4}{dt} = Wn_3 n_3 - k_4 n_4. \tag{8}$$

With the assumptions as above the approximate solutions to these rate equations are

$$n_3(t) = n_3(0)\exp(-k_3 t), \tag{9}$$

$$n_4(t) = \frac{n(0)^2 W}{k_4 - 2k_3}\left[\exp(-2k_3 t) - \exp(-k_4 t)\right]. \tag{10}$$

For Process (3) the excited state absorption occurs within the time of the laser pulse which is smaller than 7 ns and therefore no measurable rise time is expected for the build-up in the population of the $^2G_{7/2}$ state. Excited state absorption within the same laser pulse is not expected from any state lower than $^4F_{9/2}$ state since there is no significant population of these states within the 7 ns laser pulse. Note that the repetition rate of the laser was slow enough so that the long lived excited states were not populated from a second laser pulse.

The decay curves of the emission from the $^4G_{11/2}$ as a function of concentration show a sharp change in mechanism of the up-conversion process with concentration (Figs. 5, 6, 7). This change occurs at low temperatures between $x = 0.15$ and 0.25. At higher temperatures this change in behaviour occurs at higher concentrations.

To distinguish between these processes, we have attempted to model the predicted time evolution of the emission and compare it with the experimental results. Figure 8 shows the time evolution of the emission from the $^4G_{11/2}$ state for the $x = 1$ crystal at 80 K, compared with the calculated decay curve for Process (1). The agreement is excellent considering the approximations involved and that *there is no curve fitting*, the rates k_2 and k_3 having been directly measured previously. Provided that k_4 is large enough that the denominators in the bracketed terms in Eq. (6) have the same sign then the decay curves are almost independent of k_4. The agreement between the a priori calculated curves and the experimental data strongly suggests that Process (1) is dominant in this concentration and temperature regime. Models based on Process (2) fail to reproduce the experimental data in this regime.

For $x = 0.1$ the decay curves and hence the mechanism is clearly different. There is still a finite rise time which eliminates excited state absorption as a

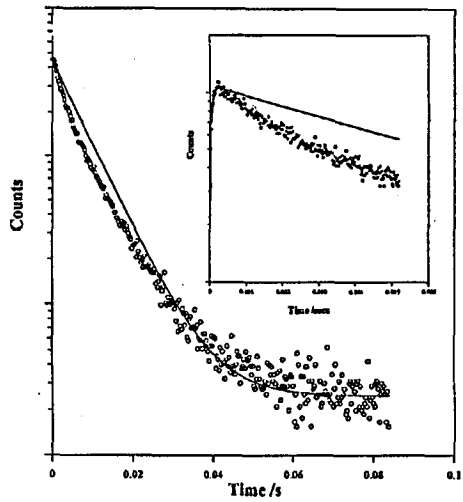

Fig. 9. 80 K ultraviolet luminescence decay curves (measured at 25974 cm^{-1}) with excitation at 15360 cm^{-1} for $Cs_2NaEr_{0.1}Y_{0.9}Cl_6$. The solid line was calculated a priori using Eq. (10). The inset shows the short time behaviour.

possible mechanism. The calculated curves based on Process (1) fail to predict the time evolution of the emission for this concentration. However a priori calculated decay curves based on Process (2) (using the separately measured values of k_3) have a general resemblance to the measured data but the decay following the initial rise is faster than predicted (Fig. 9). A possible explanation is the neglect of the third term in Eq. (7) which will lead to enhanced depopulation of state 3 when n_3 is relatively large, i.e. during the early part of the decay curve.

6. Conclusions

Excitation into the $^4F_{9/2}$ state of Er^{3+} in $Cs_2NaEr_xY_{1-x}Cl_6$ ($x = 0.001 \div 1$) results in strong emission from this level with little cross relaxation even for $x = 1$. This state decays to the remarkably long lived $^4I_{9/2}$ state which has an emissive lifetime of 0.125 s. Up-conversion processes involving both these states lead to emission in the ultraviolet region. The kinetics of the decay curves from the state populated by up-conversion shows that for $x = 1$ both the $^4F_{9/2}$ and $^4I_{9/2}$ states are involved whereas at low concentrations only the $^4F_{9/2}$ state is responsible.

We thank the EPSRC for the award of a postgraduate grant to MC.

References

[1] Z. Hasan, F.S. Richardson, *Molec. Phys.* 45, 1299 (1982).

[2] P.A. Tanner, *Molec. Phys.* 63, 365 (1988).

[3] W. Ryba-Romanowski, Z. Mazurak, B. Jeżowska-Trzebiatowska, *J. Lumin.* 27, 177 (1982).

[4] W. Ryba-Romanowski, G. Dominiak-Dzik, S. Golab, *J. Phys., Condens. Matter* 6, 1593 (1992).

[5] M. Bettinelli, C.D. Flint, *J. Phys., Condens. Matter* **2**, 8417 (1990).

[6] S.O. Vasquez, C.D. Flint, *Chem. Phys. Lett.* **238**, 378 (1995).